INSTITUT FÜR INFORMATIK

UND PRAKTISCHE MATHEMATIK

Structure Multivector for Local Analysis of Images

Michael Felsberg and Gerald Sommer

Bericht Nr. 2001
Februar 2000

CHRISTIAN-ALBRECHTS-UNIVERSITÄT

KIEL

Institut für Informatik und Praktische Mathematik der
Christian-Albrechts-Universität zu Kiel
Olshausenstr. 40
D – 24098 Kiel

Structure Multivector for Local Analysis of Images

Michael Felsberg and Gerald Sommer

Bericht Nr. 2001
Februar 2000

e-mail: mfe@ks.informatik.uni-kiel.de

This work has been supported by German National Merit Foundation and by DFG Graduiertenkolleg No. 357 (M. Felsberg) and by DFG Grant So-320-2-2 (G. Sommer).

Abstract

The structure multivector is a new approach for analyzing the local properties of a two-dimensional signal (e.g. images). It combines the classical concepts of the structure tensor and the analytic signal in a new way. This has been made possible by using a representation in the algebra of quaternions. The resulting method is linear and of low complexity. The filter-response includes local phase, local amplitude and local orientation of intrinsically one-dimensional neighborhoods in the signal. As for the structure tensor, the structure multivector field can be used to apply special filters to it for detecting two-dimensional features like corners. Experiments and comparisons with other approaches have been made.

Contents

1 Introduction

In image and image sequence processing, different paradigms of interpreting the signals exist. Regardless of they are following a constructive or an appearance based strategy, they all need a capable low-level preprocessing scheme. One of the surely most discussed topics is the detection of key points, or points of higher intrinsic dimension (in the context of appearance based approaches one should better talk of representation than of detection). Key points are needed for solving the correspondence problem occuring in 3D reconstruction, for applying steerable filters (see e.g. [16, 20]), for all kinds of model based representations, etc..

Since the preprocessing is only the first link in a long chain of operations, it is useful to have a linear approach, because otherwise it would be nearly impossible to design the higher-level processing steps. On the other hand, we need a rich representation if we want to treat as much as possible in the preprocessing. Furthermore, the representation of the signal during the different operations should be complete, in order to prevent a loss of information. These constraints enforce us to use the framework of geometric algebra which is also advantageous if we combine image processing with neural computing and robotics (see [18]).

The representation of points with special intrinsic dimensionality needs a mathematical treatment of the relevant data, which means that structural information has to be separated from textures and noise. In the one-dimensional case, quadrature filters are a frequently used approach for processing data. But the standard extension to two dimensions is not very efficient because it closely depends on the preference direction of the filter.

The structure tensor (see e.g. [13]) is a capable approach for detecting the existence and orientation of local, intrinsic one-dimensional neighborhoods. From the tensor field the orientation vector field can be constructed and by a normalized or differential convolution special symmetries can be detected (see e.g. [14]). The structure tensor itself can be computed with quadrature filters (see [10]) but the tensor itself does not possess the typical properties of a quadrature filter. Especially the linearity and the split of the identity is lost, because the phase is neglected.

In this report, we introduce a new approach for the 2D analytic signal which enables us to substitute the structure tensor by an entity which is linear, preserves the split of the identity and has a geometrically meaningful representation: the structure multivector.

2 A new approach for the 2D analytic signal

In the first section, we repeat some fundamentals, in order to make the new concepts easier to understand. In the following sections, we introduce the new approach for the analytic signal in two steps. Firstly, we define the coordinate system, in which we work in the sequel and which also follows directly from geometric constraints. Secondly, the spherical analytic signal is defined using the introduced coordinate system.

2.1 Fundamentals

Since we work on images, which can be treated as sampled intervals of $\mathbb{R}^2$, we use the geometric algebra $\mathbb{R}_{0,2}$ which is isomorphic to the algebra of quaternions $\mathbb{H}$. The whole complex signal theory naturally embeds in the algebra of quaternions, e.g. complex numbers are considered as a subspace of quaternions here. The basis of the quaternions reads $\{\mathbf{1}, \boldsymbol{i}, \boldsymbol{j}, \boldsymbol{k}\}$ while the basis of the complex numbers reads $\{\mathbf{1}, \boldsymbol{i}\}$. Normally, the basis vector $\mathbf{1}$ is omitted.

Throughout this document, we use the following notations:

- in contrast to multivectors, vectors (1D and 2D) are bold face $\boldsymbol{x} = x_1\boldsymbol{i} + x_2\boldsymbol{j}$, $\boldsymbol{u} = u_1\boldsymbol{i} + u_2\boldsymbol{j}$, $\boldsymbol{t} = t\boldsymbol{i}$, etc. and 2D vectors have the directions φ_x, φ_u, etc.
- the Fourier transform of the nD signal $f(\boldsymbol{x})$ is denoted

$$f(\boldsymbol{x}) \circ\!\!-\!\!\bullet F(\boldsymbol{u}) = \int_{\mathbb{R}^n} f(\boldsymbol{x}) \exp(-i2\pi\boldsymbol{u}\cdot\boldsymbol{x})\, d\boldsymbol{x}$$

- the real part, the $\boldsymbol{i}$-part, the $\boldsymbol{j}$-part, and the $\boldsymbol{k}$-part of a quaternion q is obtained by $\mathcal{R}\{q\}$, $\mathcal{I}\{q\}$, $\mathcal{J}\{q\}$, and $\mathcal{K}\{q\}$, respectively
- the automorphisms of the quaternions are denoted by $\alpha(q) = -\boldsymbol{i}q\boldsymbol{i}$, $\beta(q) = -\boldsymbol{j}q\boldsymbol{j}$, and $\gamma(q) = -\boldsymbol{k}q\boldsymbol{k}$, where the conjugation of the complex numbers can be expressed either by $\beta(z)$ or by $\gamma(z)$ ($z = \mathcal{R}\{z\} + \mathcal{I}\{z\}\boldsymbol{i}$)

The 1D analytic signal can be defined as follows (see e.g. [13]). The signal which is obtained from $f(\boldsymbol{x})$ by a phase shift of $\pi/2$ is called the Hilbert transform $f_H(\boldsymbol{x})$ of $f(\boldsymbol{x})$. Since $f_H(\boldsymbol{x})$ shall be real-valued, the spectrum must have an odd symmetry. Therefore, the transfer function has the form[1]

$$H(\boldsymbol{u}) = \boldsymbol{i}\,\mathrm{sign}(\boldsymbol{u}) \quad . \tag{1}$$

[1]Since we use vector notation for 1D functions, we have to redefine some real-valued functions according to $\mathrm{sign}(\boldsymbol{u}) = \mathrm{sign}(u)$, where $\boldsymbol{u} = u\boldsymbol{i}$.

If we combine a signal and its Hilbert transform corresponding to

$$f_A(\boldsymbol{x}) = f(\boldsymbol{x}) - f_H(\boldsymbol{x})\boldsymbol{i} \quad , \tag{2}$$

we get a complex-valued signal, which is called the analytic signal of $f(\boldsymbol{x})$.

According to (1), the Fourier transform of the analytic signal $f_A(\boldsymbol{x})$ is located in the right half-space of the frequency domain:

$$f_A(\boldsymbol{x}) \circ\!\!-\!\!\bullet F(\boldsymbol{u}) - \boldsymbol{i}\,\mathrm{sign}(\boldsymbol{u})F(\boldsymbol{u})\boldsymbol{i} = \begin{cases} 2F(\boldsymbol{u}) & \text{if } \boldsymbol{u}\boldsymbol{i} < 0 \\ F(0) & \text{if } \boldsymbol{u} = 0 \\ 0 & \text{if } \boldsymbol{u}\boldsymbol{i} > 0 \end{cases} \tag{3}$$

Hence, we have recalled all facts of the one-dimensional analytic signal which are relevant for this report. More information can be found in any good textbook about signal-theory.

Since we use the algebra of quaternions as a geometric algebra, we have to introduce some terms of geometric algebra (for a complete introduction, see e.g. [12]). If the algebra of quaternions is identified with the geometric algebra $\mathbb{R}_{0,2}$, the real part is also called the *scalar*, the entity consisting of $\boldsymbol{i}$- and $\boldsymbol{j}$-parts is called the *vector* and the $\boldsymbol{k}$-part is called the *bivector* ($\boldsymbol{k} = \boldsymbol{i}\boldsymbol{j}$).

We have already used two products: the inner product, e.g. $\boldsymbol{x} \cdot \boldsymbol{u}$, and the geometric product, e.g. $\boldsymbol{u}\boldsymbol{i}$. The geometric product is evaluated by applying the associative law and the multiplication table of the algebra. The inner product is well known for vectors, but it can be extended to elements of all grades (geometric algebras are graded algebras) by

$$A \cdot B = \langle AB \rangle_{|r-s|} \tag{4}$$

where $<>$ is the grade operator and $A = \langle A \rangle_r$ and $B = \langle B \rangle_s$. The inner product with a scalar is always zero.

The outer product is defined by

$$A \wedge B = \langle AB \rangle_{r+s} \tag{5}$$

which yields the identity $\boldsymbol{x} \wedge \boldsymbol{u} = \boldsymbol{x}\boldsymbol{u} - \boldsymbol{x} \cdot \boldsymbol{u}$ for vectors. If at least one factor is a scalar, the outer product is identical to the geometric product respective the field multiplication.

A rotation in 2D vector space can be expressed by a *spinor*, in the case of quaternions for example, we have a scalar s, a vector $\boldsymbol{x} = x_1\boldsymbol{i} + x_2\boldsymbol{j}$ and a bivector $b\boldsymbol{k}$. Together, they form the quaternion $q = s + \boldsymbol{x} + b\boldsymbol{k}$. If we want to rotate the vector (and only the vector)

by φ, this can be done by the spinor $\exp(\boldsymbol{k}\varphi/2)$:

$$\begin{aligned}
\exp(\boldsymbol{k}\varphi/2)q\exp(-\boldsymbol{k}\varphi/2) &= s + \exp(\boldsymbol{k}\varphi/2)\boldsymbol{x}\exp(-\boldsymbol{k}\varphi/2) + b\boldsymbol{k} \\
&= s + ((\cos(\varphi/2)x_1 - \sin(\varphi/2)x_2)\boldsymbol{i} + \\
&\quad (\cos(\varphi/2)x_2 + \sin(\varphi/2)x_1)\boldsymbol{j})\exp(-\boldsymbol{k}\varphi/2) + b\boldsymbol{k} \\
&= s + (\cos^2(\varphi/2)x_1 - 2\cos(\varphi/2)\sin(\varphi/2)x_2 - \sin^2(\varphi/2)x_1)\boldsymbol{i} + \\
&\quad (2\cos(\varphi/2)\sin(\varphi/2)x_1 - \sin^2(\varphi/2)x_2 + \cos^2(\varphi/2)x_2)\boldsymbol{j} + b\boldsymbol{k} \\
&= s + (x_1\cos(\varphi) - x_2\sin(\varphi))\boldsymbol{i} + (x_1\sin(\varphi) + x_2\cos(\varphi))\boldsymbol{j} + b\boldsymbol{k}
\end{aligned}$$

2.2 The 2D phase concept

We want to develop a new 2D analytic signal for intrinsically 1D signals (in contrast to the 2D analytic signal in [4] which is designed for intrinsically 2D signals), which shall include three properties: local amplitude, local phase and local orientation. Compared to the 1D analytic signal we need one additional phase. We cannot choose this phase without constraints: if the signal is rotated by π, we obtain the same analytic signal, but conjugated. Therefore, we have the following relationship: negation of the local phase is identical to a rotation of π.

One straightforward consequence is that points where the analytic signal has zero phase (i.e. it is real-valued) have orientation φ_u and $\varphi_u + \pi$ at the same time - therefore, these points have no orientation at all. Note the difference between *direction* and *orientation* in this context; the direction is a value in $[0; 2\pi)$ and the orientation is a value in $[0; \pi)$ (see [9]).

A second consequence is the following. Any value of the 2D analytic signal can be understood as a 3D vector. The amplitude fixes the sphere on which the value is located. The local phase corresponds to rotations on a great circle on this sphere. To be consistent, a rotation of the signal must then correspond to a rotation on a small circle.

An obvious parameterization is the following: assuming that we have a complex-valued function over a two-dimensional domain, we map the imaginary unit onto the normalized position vector (the direction vector). The resulting function is quaternion-valued and has the following properties:

- If we choose one fixed orientation φ_u in the right half-space, the imaginary unit is changed into $(\cos(\varphi_u)\boldsymbol{i} + \sin(\varphi_u)\boldsymbol{j})\,\mathrm{sign}(u_1)$.
- For every orientation, the function lies on a different complex plane (note that every algebra over $\{\mathbf{1}, q_0\}$, q_0 a pure unit quaternion, is isomorphic to the algebra of complex numbers). The phase in this plane is denoted φ_i.
- The values of the function include information about the orientation of the function.

The coordinate system defined in this way is displayed in figure 1. It is the same

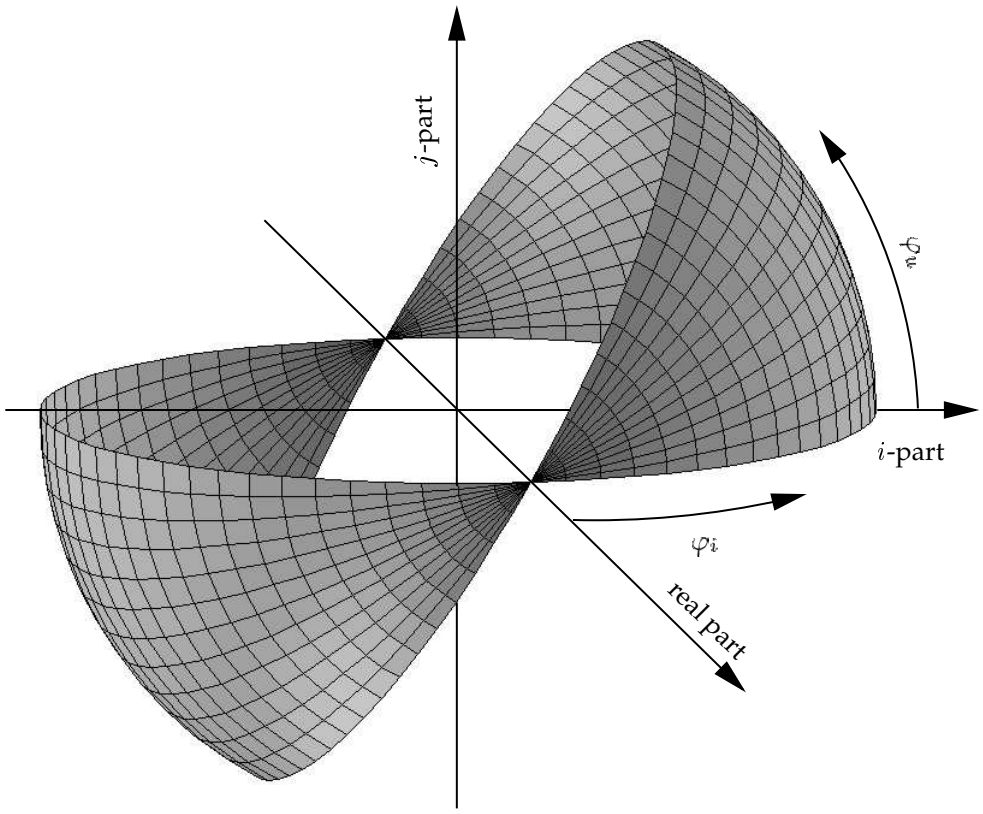

Figure 1: Coordinate system of the 2D phase approach

as in [10], but Granlund and Knutsson use the 2D phase in the context of orientation adaptive filtering (see also [11]).

Consider a given quaternion q, how can we extract the two phases, described just above? In fact, the answer of this question defines the introduced coordinate system.

Definition 1 *Let* $\arg(z)$ *be the function which evaluates the complex phase of* z *in the interval* $[0; 2\pi)$ *and let* q_s *be a quaternion with zero* k *part. Then, we get the orientation phase* φ_u *by*

$$\varphi_u = \arg((\mathcal{I}\{q_s\} + \mathcal{J}\{q_s\}\boldsymbol{i})^2)/2 \ , \tag{6}$$

and the phase in the complex subspace spanned by $\mathbf{1}$ *and* $\cos(\varphi_u)\boldsymbol{i} + \sin(\varphi_u)\boldsymbol{j}$ *is obtained by*

$$\begin{aligned} \varphi_i &= \arg(\mathcal{R}\{q_s\} + (\mathcal{I}\{q_s\} + \mathcal{J}\{q_s\}\boldsymbol{i})\exp(-\boldsymbol{i}\varphi_u)\boldsymbol{i}) \\ &= \arg(\mathcal{R}\{q_s\} - (\mathcal{J}\{q_s\} - \mathcal{I}\{q_s\}\boldsymbol{i})\exp(-\boldsymbol{i}\varphi_u)) \ . \end{aligned} \tag{7}$$

Note that these definitions of quaternionic phases are totally different from those of the quaternionic Fourier transform (see e.g. [4]). The reason why we use a different phase will be explained at the end of section 2.3.

2.3 The spherical analytic signal

Now, having a phase concept which is rich enough to code all local properties of intrinsically one-dimensional signals, we construct a generalized Hilbert transform and an analytic signal for the 2D case, which make use of the new embedding.

The following definition of the spherical Hilbert transform is motivated by theorem 1, which establishes a correspondence between the Hilbert transform and the spherical Hilbert transform.

Definition 2 *Let* $F(\boldsymbol{u})$ *be the Fourier transform of* $f(\boldsymbol{x})$*. Then the* spherical Hilbert transform *of* $f(\boldsymbol{x})$ *is defined in the Fourier domain by*

$$F_H(\boldsymbol{u}) = \tilde{H}(\boldsymbol{u})F(\boldsymbol{u}) = \frac{\boldsymbol{u}}{|\boldsymbol{u}|}F(\boldsymbol{u}) \ , \tag{8}$$

and $F_H(\boldsymbol{u}) \bullet\!\!-\!\!\circ\, f_H(\boldsymbol{x})$.

Note that the operator $\tilde{H}(\boldsymbol{u})$ has to be applied from the left. In section 3.1, it will be shown that the components of the spherical Hilbert transform are identical to the Riesz transform.

Example 1:

$f(\boldsymbol{x}) = \cos(2\pi \boldsymbol{u}_0 \cdot \boldsymbol{x})$

$$\begin{aligned} F_H(\boldsymbol{u}) &= \tilde{H}(\boldsymbol{u}) \frac{\delta_0(\boldsymbol{u}-\boldsymbol{u}_0) + \delta_0(\boldsymbol{u}+\boldsymbol{u}_0)}{2} \\ &= \frac{\boldsymbol{u}\delta_0(\boldsymbol{u}-\boldsymbol{u}_0) + \boldsymbol{u}\delta_0(\boldsymbol{u}+\boldsymbol{u}_0)}{2|\boldsymbol{u}|} \\ &= \frac{\boldsymbol{u}_0\delta_0(\boldsymbol{u}-\boldsymbol{u}_0) - \boldsymbol{u}_0\delta_0(\boldsymbol{u}+\boldsymbol{u}_0)}{2|\boldsymbol{u}_0|} \\ &= \frac{\boldsymbol{u}_0}{|\boldsymbol{u}_0|}\boldsymbol{i}\,\frac{\delta_0(\boldsymbol{u}-\boldsymbol{u}_0) - \delta_0(\boldsymbol{u}+\boldsymbol{u}_0)}{2\boldsymbol{i}} \quad , \end{aligned}$$

so that $F_H(\boldsymbol{u}) \bullet\!\!-\!\!\circ\; -\exp(\boldsymbol{k}\varphi_0)\sin(2\pi \boldsymbol{u}_0 \cdot \boldsymbol{x})$, where $\varphi_0 = \arg(\boldsymbol{u}_0)$.

Example 2:

$f(\boldsymbol{x}) = \sin(2\pi \boldsymbol{u}_0 \cdot \boldsymbol{x})$

$$F_H(\boldsymbol{u}) = -\frac{\boldsymbol{u}_0}{|\boldsymbol{u}_0|}\boldsymbol{i}\,\frac{\delta_0(\boldsymbol{u}-\boldsymbol{u}_0) + \delta_0(\boldsymbol{u}+\boldsymbol{u}_0)}{2} \quad ,$$

so that $F_H(\boldsymbol{u}) \bullet\!\!-\!\!\circ\; \exp(\boldsymbol{k}\varphi_0)\cos(2\pi \boldsymbol{u}_0 \cdot \boldsymbol{x})$.

Obviously, the spherical Hilbert transform yields functions which are identical to the 1D Hilbert transforms of the cosine and sine function, respectively, except for an additional exponential function.

Up to now, we have only considered two special examples, but what about general signals? What kind of signals can be treated with this approach? The answer can be found easily: the orientation phase must be independent of the frequency coordinate. This sounds impossible, but in fact, the orientation phase is constant, if the spectrum is located on a line through the origin.

Signals which have a spectrum of this form are intrinsically one-dimensional (i.e. they are constant in one direction). This is exactly the class of functions for which the structure tensor has been designed. For these functions we have the following theorem:

Theorem 1 *Let $f(\boldsymbol{t})$ be a one-dimensional function with the Hilbert transform $f_H(\boldsymbol{t})$. Then, the spherical Hilbert transform of the two-dimensional function $f'(\boldsymbol{x}) = f((\boldsymbol{x}\cdot\boldsymbol{n})\boldsymbol{i})$ reads $f'_H(\boldsymbol{x}) = -\boldsymbol{n}\boldsymbol{i}\, f_H((\boldsymbol{x}\cdot\boldsymbol{n})\boldsymbol{i})$, where $\boldsymbol{n} = \cos(\theta)\boldsymbol{i} + \sin(\theta)\boldsymbol{j}$ is an arbitrary unit vector.*

Proof:

The Fourier transform of $f'(\boldsymbol{x})$ reads $F((\boldsymbol{u}\cdot\boldsymbol{n})\boldsymbol{i})\delta_0(\boldsymbol{u}\wedge\boldsymbol{n})$ if $f(\boldsymbol{t}) \circ\!\!-\!\!\bullet F(\boldsymbol{s})$. Corresponding to (8) we obtain

$$\frac{\boldsymbol{u}}{|\boldsymbol{u}|}F((\boldsymbol{u}\cdot\boldsymbol{n})\boldsymbol{i})\delta_0(\boldsymbol{u}\wedge\boldsymbol{n}) = \boldsymbol{n}\,\mathrm{sign}(\boldsymbol{u}\cdot\boldsymbol{n})F((\boldsymbol{u}\cdot\boldsymbol{n})\boldsymbol{i})\delta_0(\boldsymbol{u}\wedge\boldsymbol{n})$$

and we can take the term $\boldsymbol{n}$ in the inverse Fourier transform outside the integral:

$$\begin{aligned}
&\int_{\mathbb{R}^2} \boldsymbol{n}\,\mathrm{sign}(\boldsymbol{u}\cdot\boldsymbol{n})F((\boldsymbol{u}\cdot\boldsymbol{n})\boldsymbol{i})\delta_0(\boldsymbol{u}\wedge\boldsymbol{n})\exp(i2\pi\boldsymbol{u}\cdot\boldsymbol{x})\,d\boldsymbol{u} \\
&\qquad = -\boldsymbol{n}\boldsymbol{i}\int_{\mathbb{R}^2} \mathrm{sign}(\boldsymbol{u}\cdot\boldsymbol{n})F((\boldsymbol{u}\cdot\boldsymbol{n})\boldsymbol{i})\delta_0(\boldsymbol{u}\wedge\boldsymbol{n})\exp(i2\pi\boldsymbol{u}\cdot\boldsymbol{x})\,d\boldsymbol{u} \\
&\qquad = -\boldsymbol{n}\boldsymbol{i}\int_{\mathbb{R}} \mathrm{sign}(\lambda)F(\lambda\boldsymbol{i})\exp(i2\pi\lambda\boldsymbol{n}\cdot\boldsymbol{x})\,d\lambda \\
&\qquad = -\boldsymbol{n}\boldsymbol{i}\, f_H((\boldsymbol{n}\cdot\boldsymbol{x})\boldsymbol{i}) \ ,
\end{aligned}$$

and therefore,

$$f'_H(\boldsymbol{x}) = -\boldsymbol{n}\boldsymbol{i}\, f_H((\boldsymbol{x}\cdot\boldsymbol{n})\boldsymbol{i}) = \exp(\boldsymbol{k}\theta) f_H((\boldsymbol{x}\cdot\boldsymbol{n})\boldsymbol{i}) \ .$$

□

Now we simply adapt (2) for the 2D case and obtain:

Definition 3 *The* spherical analytic signal *of a 2D signal $f(\boldsymbol{x})$ is obtained by*

$$f_A(\boldsymbol{x}) = f(\boldsymbol{x}) - f_H(\boldsymbol{x})\boldsymbol{i} \ , \tag{9}$$

where $f_H(\boldsymbol{x})$ is the spherical Hilbert transform of $f(\boldsymbol{x})$.

Using this definition, we obtain for our two examples:

$$\begin{aligned}
\cos(2\pi\boldsymbol{u}_0\cdot\boldsymbol{x}) + \exp(\boldsymbol{k}\varphi_0)\sin(2\pi\boldsymbol{u}_0\cdot\boldsymbol{x})\boldsymbol{i} &= \cos(2\pi\boldsymbol{u}_0\cdot\boldsymbol{x}) + \frac{\boldsymbol{u}_0}{|\boldsymbol{u}_0|}\sin(2\pi\boldsymbol{u}_0\cdot\boldsymbol{x}) \\
&= \exp(\frac{\boldsymbol{u}_0}{|\boldsymbol{u}_0|}2\pi\boldsymbol{u}_0\cdot\boldsymbol{x}) \qquad \text{and} \\
\sin(2\pi\boldsymbol{u}_0\cdot\boldsymbol{x}) - \exp(\boldsymbol{k}\varphi_0)\cos(2\pi\boldsymbol{u}_0\cdot\boldsymbol{x})\boldsymbol{i} &= \sin(2\pi\boldsymbol{u}_0\cdot\boldsymbol{x}) - \frac{\boldsymbol{u}_0}{|\boldsymbol{u}_0|}\cos(2\pi\boldsymbol{u}_0\cdot\boldsymbol{x}) \\
&= \exp(\frac{\boldsymbol{u}_0}{|\boldsymbol{u}_0|}(2\pi\boldsymbol{u}_0\cdot\boldsymbol{x} - \pi/2)) \ .
\end{aligned}$$

So the spherical analytic signal uses the phase concept, which has been defined in section 2.2. According to theorem 1, the spherical analytic signal of an intrinsically one-dimensional signal $f'(\boldsymbol{x}) = f((\boldsymbol{x}\cdot\boldsymbol{n})\boldsymbol{i})$ reads

$$f'_A(\boldsymbol{x}) = f((\boldsymbol{x}\cdot\boldsymbol{n})\boldsymbol{i}) - \boldsymbol{n}f_H((\boldsymbol{x}\cdot\boldsymbol{n})\boldsymbol{i}) \ . \tag{10}$$

Of course, the spherical analytic signal can be computed for *all* functions which are Fourier transformable. However, for signals which do not have an intrinsic dimension of one[2], the correspondence to the 1D analytic signal is lost.

Independently of the intrinsic dimensionality of the signal, the analytic signal can also be calculated in a different way. The 1D analytic signal can be obtained in the Fourier domain by the transfer function $1 + \mathrm{sign}(\boldsymbol{u})$. For the spherical analytic signal we have the same result if we modify the Fourier transform.

Definition 4 *The* inverse spherical Fourier transform *of $F(\boldsymbol{u})$ is defined by*

$$\tilde{f}(\boldsymbol{x}) = \int_{\mathbb{R}^2} \exp(\boldsymbol{k}\varphi_u/2) F(\boldsymbol{u}) \exp(\boldsymbol{i}2\pi\boldsymbol{u}\cdot\boldsymbol{x}) \exp(-\boldsymbol{k}\varphi_u/2)\, d\boldsymbol{u} \quad . \tag{11}$$

Before we investigate the inverse of this transform and some of its properties, we establish a relation between the spherical analytic signal and the inverse spherical Fourier transform:

Theorem 2 *The spherical analytic signal of $f(\boldsymbol{x})$ is the inverse spherical Fourier transform of $F(\boldsymbol{u})$.*

Proof:

The inverse Fourier transform of $(1 - \frac{\boldsymbol{u}}{|\boldsymbol{u}|}\boldsymbol{i})F(\boldsymbol{u})$ can be calculated by an integration over $\boldsymbol{u}$ or $-\boldsymbol{u}$, the integrals are identical. Therefore, we have

$$\begin{aligned}
f_A(\boldsymbol{x}) &= \int_{\mathbb{R}^2} (1 - \frac{\boldsymbol{u}}{|\boldsymbol{u}|}\boldsymbol{i}) F(\boldsymbol{u}) \exp(\boldsymbol{i}2\pi\boldsymbol{u}\cdot\boldsymbol{x})\, d\boldsymbol{u} \\
&= \frac{1}{2}\int_{\mathbb{R}^2} (1 - \frac{\boldsymbol{u}}{|\boldsymbol{u}|}\boldsymbol{i}) F(\boldsymbol{u}) \exp(\boldsymbol{i}2\pi\boldsymbol{u}\cdot\boldsymbol{x}) + (1 + \frac{\boldsymbol{u}}{|\boldsymbol{u}|}\boldsymbol{i}) F^*(\boldsymbol{u}) \exp(-\boldsymbol{i}2\pi\boldsymbol{u}\cdot\boldsymbol{x})\, d\boldsymbol{u} \\
&= \int_{\mathbb{R}^2} \mathcal{R}\{F(\boldsymbol{u}) \exp(\boldsymbol{i}2\pi\boldsymbol{u}\cdot\boldsymbol{x})\} + \frac{\boldsymbol{u}}{|\boldsymbol{u}|}\mathcal{I}\{F(\boldsymbol{u}) \exp(\boldsymbol{i}2\pi\boldsymbol{u}\cdot\boldsymbol{x})\}\, d\boldsymbol{u} \\
&= \int_{\mathbb{R}^2} \exp(\boldsymbol{k}\varphi_u/2) F(\boldsymbol{u}) \exp(\boldsymbol{i}2\pi\boldsymbol{u}\cdot\boldsymbol{x}) \exp(-\boldsymbol{k}\varphi_u/2)\, d\boldsymbol{u} \\
&= \tilde{f}(\boldsymbol{x}) \quad .
\end{aligned}$$

□

[2]The case of intrinsic dimension zero (i.e. a constant signal) is irrelevant, because the Hilbert transform is zero in both cases.

Above, we mentioned that the spherical analytic signal can be obtained by a similar transfer function as in the 1D case if the modified Fourier transform is used. Up to now, we used the whole spectrum, but since

$$\begin{aligned}
&\exp(\boldsymbol{k}\varphi_u/2)F(\boldsymbol{u})\exp(\boldsymbol{i}2\pi\boldsymbol{u}\cdot\boldsymbol{x})\exp(-\boldsymbol{k}\varphi_u/2)\\
&\quad=\exp(\boldsymbol{k}(\varphi_u+\pi)/2)\boldsymbol{k}F^*(-\boldsymbol{u})(\exp(-\boldsymbol{i}2\pi\boldsymbol{u}\cdot\boldsymbol{x}))^*(-\boldsymbol{k})\exp(-\boldsymbol{k}(\varphi_u+\pi)/2)\\
&\quad=\exp(\boldsymbol{k}(\varphi_u+\pi)/2)\gamma((F(-\boldsymbol{u})\exp(-\boldsymbol{i}2\pi\boldsymbol{u}\cdot\boldsymbol{x}))^*)\exp(-\boldsymbol{k}(\varphi_u+\pi)/2)\\
&\quad=\exp(\boldsymbol{k}(\varphi_u+\pi)/2)F(-\boldsymbol{u})\exp(-\boldsymbol{i}2\pi\boldsymbol{u}\cdot\boldsymbol{x})\exp(-\boldsymbol{k}(\varphi_u+\pi)/2)\ ,
\end{aligned}$$

i.e., the integrand is symmetric, we can also integrate over the half domain and multiply the integral by two. Therefore, we can use any transfer function of the form $1+\operatorname{sign}(\boldsymbol{u}\cdot\boldsymbol{n})$ without changing the integral. The most workable cases are those where $\boldsymbol{n}=\boldsymbol{i}$ or $\boldsymbol{n}=\boldsymbol{j}$. By simply omitting half of the data, the redundancy in the representation is removed.

The inverse of the transform defined by (11) is the transform which takes a spherical analytic signal and returns the classical complex spectrum. Since the original signal is simply the real part of the analytic signal, we have

$$\mathcal{R}\{\tilde{f}(\boldsymbol{x})\}\circ\!\!-\!\!\bullet F(\boldsymbol{u})\ . \tag{12}$$

In order to calculate the energy of the spherical analytic signal, we firstly need the transfer function, which changes $F(\boldsymbol{u})$ to $F_A(\boldsymbol{u})$: it is obtained from (8) and (9) and reads $1-\frac{\boldsymbol{u}}{|\boldsymbol{u}|}\boldsymbol{i}=1+\cos(\varphi_u)+\sin(\varphi_u)\boldsymbol{k}$. The energy of the spherical analytic signal is

$$\begin{aligned}
&\int_{\mathbb{R}^2}|(1+\cos(\varphi_u)+\sin(\varphi_u)\boldsymbol{k})F(\boldsymbol{u})|^2\,d\boldsymbol{u}\\
&\qquad=\int_{\mathbb{R}^2}(1+\cos(\varphi_u))^2|F(\boldsymbol{u})|^2+\sin^2(\varphi_u)|F(\boldsymbol{u})|^2\,d\boldsymbol{u}\\
&\qquad=\int_{\mathbb{R}^2}2(1+\cos(\varphi_u))|F(\boldsymbol{u})|^2\,d\boldsymbol{u}\\
&\qquad\text{and since } |F(\boldsymbol{u})|=|F(-\boldsymbol{u})|\\
&\qquad=\int_{\mathbb{R}^2}(1+\cos(\varphi_u))|F(\boldsymbol{u})|^2+(1-\cos(\varphi_u))|F(\boldsymbol{u})|^2\,d\boldsymbol{u}\\
&\qquad=2\int_{\mathbb{R}^2}|F(\boldsymbol{u})|^2\,d\boldsymbol{u}\ ,
\end{aligned}$$

i.e. it is two times the energy of the original signal[3].

From the group of similarity transformations (i.e. shifts, rotations and dilations) only the rotation really affects the spherical analytic signal; the orientation phase is changed according to the rotation. If we interpret the spherical analytic signal as a vector field

[3]This is only valid for DC free signals. The energy of the DC component is not doubled as in the case of the 1D analytic signal.

in 3D (see also section 3.2), the group of 2D similarity transforms[4] even commutes with the operator which yields the spherical analytic signal.

The reader might ask, why do we use a quaternion-valued Fourier transform which differs from the QFT (see [4, 6, 7] and for a more mathematical discussion [2])? The reason is not obvious. Therefore, we will go into some detail.

The QFT covers more symmetry concepts than the complex Fourier transform. The classical transform maps a reflection at the origin onto the conjugation operator. The QFT maps a reflection at one of the axes onto one of the algebra automorphisms. This can be shown by the isomorphism between $\mathbb{C} \otimes \mathbb{C}$ and $\mathbb{C}^2$:

In the calculation of the QFT, only products of the form $\boldsymbol{ii}$, $\boldsymbol{ij}$, $\boldsymbol{ik}$, $\boldsymbol{jj}$ and $\boldsymbol{kj}$ are used, the products $\boldsymbol{ji}$, $\boldsymbol{jk}$, $\boldsymbol{ki}$ and $\boldsymbol{kk}$ never appear. Therefore, we can use the algebra $\mathbb{C} \otimes \mathbb{C}$ instead of $\mathbb{Q}$ to calculate the QFT. Moreover, we have $\mathbb{C} \otimes \mathbb{C} \cong \mathbb{C}^2$ (see e.g. [5, 8]) and consequently, we can calculate the QFT of a real signal by two complex transformations using the formula

$$F_q(\boldsymbol{u}) = F(\boldsymbol{u})\frac{\mathbf{1} - \boldsymbol{k}}{2} + F(u_1\boldsymbol{i} - u_2\boldsymbol{j})\frac{\mathbf{1} + \boldsymbol{k}}{2} \tag{13}$$

and the symmetry wrt. the axes is obvious.

In this report, we want to present an isotropic approach which means that symmetry wrt. the axes is not sufficient. Therefore, we had to design the new transform. The design of isotropic discrete filters is a quite old topic, see e.g. [3], but still current (e.g. [15]).

[4]Note that in the context of a 3D embedding, the group of 2D similarity transforms is the subgroup of the 3D transforms restricted to shifts in i or j direction, rotations around the real axis and a dilation of the i and j axes.

3 Properties of the Spherical Analytic Signal

In this section we describe some global and local aspects of the spherical analytic signal.

3.1 The spatial representation

The definition of the spherical Hilbert transform in the frequency domain can be transformed into a spatial integral transform. The transfer function (8) can be split into two functions: $\frac{u_1}{|\boldsymbol{u}|}$ and $\frac{u_2}{|\boldsymbol{u}|}$. The only thing left is to calculate the inverse Fourier transform of these two functions. In [19, 17] the transform pairs can be found:

$$\frac{x_1}{2\pi|\boldsymbol{x}|^3} \circ\!\!-\!\!\bullet\ -\boldsymbol{i}\frac{u_1}{|\boldsymbol{u}|} \quad \text{and} \tag{14}$$

$$\frac{x_2}{2\pi|\boldsymbol{x}|^3} \circ\!\!-\!\!\bullet\ -\boldsymbol{i}\frac{u_2}{|\boldsymbol{u}|} \quad . \tag{15}$$

These Fourier correspondences can also be found by direct calculation. First we try to find the inverse transform of $\frac{1}{|\boldsymbol{u}|}$. It can be obtained using the Hankel transform, see [1]:

$$\begin{aligned}
&\int_{\mathbb{R}^2} \frac{1}{|\boldsymbol{u}|} \exp \boldsymbol{i}2\pi\boldsymbol{u}\cdot\boldsymbol{x}\, d\boldsymbol{u} \\
&\qquad \text{substitute } \boldsymbol{x} = r(\cos(\theta)\boldsymbol{i} + \sin(\theta)\boldsymbol{j}) \text{ and } \boldsymbol{u} = q(\cos(\varphi)\boldsymbol{i} + \sin(\varphi)\boldsymbol{j}) \\
&\qquad = \int_0^{\infty}\int_0^{2\pi} q^{-1} \exp \boldsymbol{i}2\pi rq\cos(\varphi-\theta) q\, dq\, d\varphi \\
&\qquad \text{which is the Hankel transform of } q^{-1} \\
&\qquad = r^{-1} = |\boldsymbol{x}|^{-1} \ .
\end{aligned}$$

Now, using the derivative theorem of the Fourier transform we obtain:

$$\frac{\partial}{\partial x_1}|\boldsymbol{x}|^{-1} \circ\!\!-\!\!\bullet\ \boldsymbol{i}2\pi\frac{u_1}{|\boldsymbol{u}|}$$

and since

$$\frac{\partial}{\partial x_1}|\boldsymbol{x}|^{-1} = -\frac{x_1}{|\boldsymbol{x}|^3}$$

we obtain (14).

The functions $\frac{x_1}{2\pi|\boldsymbol{x}|^3}$ and $\frac{x_2}{2\pi|\boldsymbol{x}|^3}$ are the kernels of the 2D Riesz transform ([19]). From a mathematician's point of view, the Riesz transform is the multidimensional generalization of the Hilbert transform. From (14) and (15) we obtain

$$\frac{\boldsymbol{i}x_1}{2\pi|\boldsymbol{x}|^3} \circ\!\!-\!\!\bullet\ \frac{u_1}{|\boldsymbol{u}|} \quad \text{and} \tag{16}$$

$$\frac{\boldsymbol{i}x_2}{2\pi|\boldsymbol{x}|^3} \circ\!\!-\!\!\bullet\ \frac{u_2}{|\boldsymbol{u}|} \quad , \tag{17}$$

by the linearity of the Fourier transform

$$\frac{\boldsymbol{x}}{2\pi|\boldsymbol{x}|^3}\boldsymbol{i} \circ\!\!-\!\!\bullet \frac{\boldsymbol{u}}{|\boldsymbol{u}|} \quad . \tag{18}$$

Consequently, the spherical Hilbert transform (or the Riesz transform) of a signal $f(\boldsymbol{x})$ is obtained by convolving the signal with $\frac{\boldsymbol{x}}{2\pi|\boldsymbol{x}|^3}\boldsymbol{i}$:

$$f_H(\boldsymbol{x}) = \int_{\mathbb{R}^2} \frac{\boldsymbol{t}}{2\pi|\boldsymbol{t}|^3}\boldsymbol{i} f(\boldsymbol{x}-\boldsymbol{t})\, d\boldsymbol{t} \quad . \tag{19}$$

The spherical analytic signal is directly obtained by the convolution

$$f_A(\boldsymbol{x}) = \int_{\mathbb{R}^2} \left(\delta_0(\boldsymbol{t}) + \frac{\boldsymbol{t}}{2\pi|\boldsymbol{t}|^3}\right) f(\boldsymbol{x}-\boldsymbol{t})\, d\boldsymbol{t} \quad . \tag{20}$$

The graph in figure 2 sums up all ways to calculate the spherical analytic signal from the preceding sections. The inverse spherical Fourier transform is denoted $\mathcal{F}_s^{-1}$.

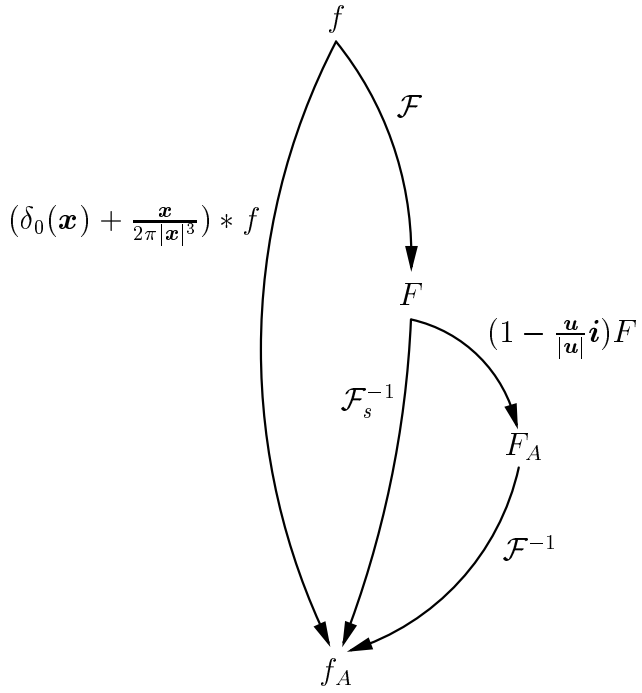

Figure 2: Three ways to calculate the spherical analytic signal

3.2 The structure multivector

Normally, images are intrinsically two-dimensional, so the concepts described in section 2.3 cannot be applied globally. On the other hand, large areas of images are intrinsically one-dimensional, at least on a certain scale. Therefore, a local processing would take advance of the new approach.

Compared to local properties of 1D signals, intrinsic one-dimensional signals only have one additional property: the local orientation. Therefore, it is quite reasonable to extend the local description by this parameter.

The classical approach of the analytic signal has its local counterpart in the quadrature filters. A pair of quadrature filters (or a complex quadrature filter) is characterized by the fact that the impulse response is an analytic signal. On the other hand, both impulse responses can be bounded (i.e. they act on a local neighborhood), so that the problem of the unlimited impulse response of the Hilbert filter is circumvented.

An example of the output of a 1D quadrature filter can be found in figure 3. While

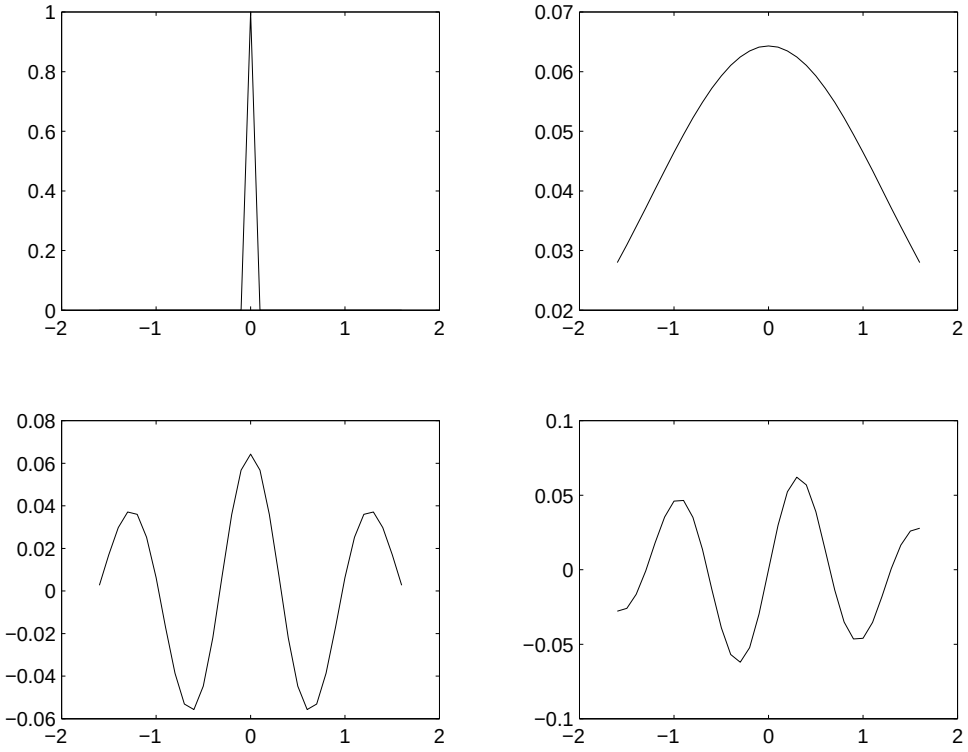

Figure 3: Upper left: impulse, upper right: magnitude of filter output, lower left: real part of filter output, lower right: imaginary part of filter output

the representation in figure 3 is very common, we will introduce now a different rep-

resentation. One-dimensional signals can be interpreted as surfaces in 2D space. If we assign the real axis to the signal values and the imaginary axis to the abscissa, we obtain a representation in the complex plane. The analytic signal can be embedded in the same plane – it corresponds to a vector field which is only non-zero on the imaginary axis (see figure 4).

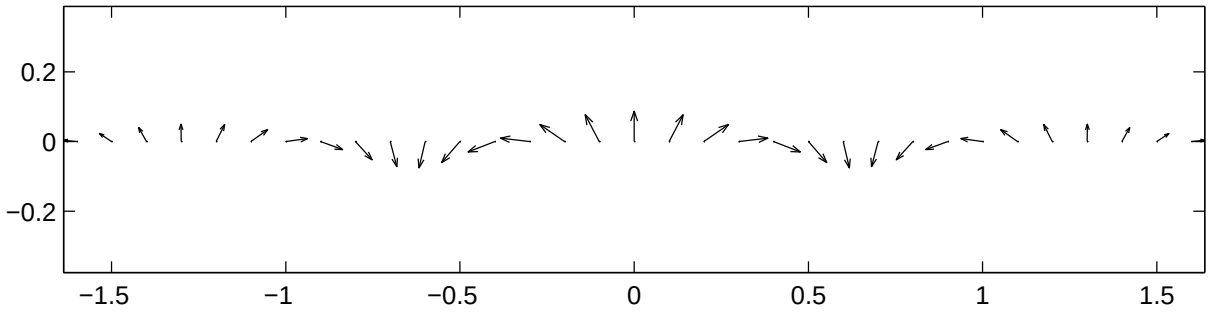

Figure 4: Representation of the 1D analytic signal as a vector field

The vector field representation of the analytic signal looks like particles which roll from a hill (impulse). The rotation is directed away from the peak and the speed (amplitude of vectors) decreases with increasing distance.

Based on the spherical analytic signal we now introduce the spherical quadrature filters. They are defined according to the 1D case.

Definition 5 *A hypercomplex filter whose impulse response is a spherical analytic signal is called a spherical quadrature filter.*

In practical applications, the convolution (20) cannot be applied directly either, because of the unlimited impulse response of the expression (20). Of course, one could create optimized filters for signals which are supposed to be band-limited, but it is better workable to use radial bandpass filters to band-limit the signal actively. The spatial representation of a radial bandpass can be used to design the spherical quadrature filter in the spatial domain. The spatial representation looks similar to a Bessel function (see figure 5). In fact, it is a linear combination of Bessel functions with different scales.

It is remarkable that the spherical quadrature filters have isotropic energy and exactly choose the frequency bands they are designed for. In figure 6 it can be seen that the energy is isotropic and that it is maximal for the radius 77.8, which corresponds to a frequency of $\frac{16.3}{256}$. The used bandpass has a center frequency of $\frac{1}{16}$.

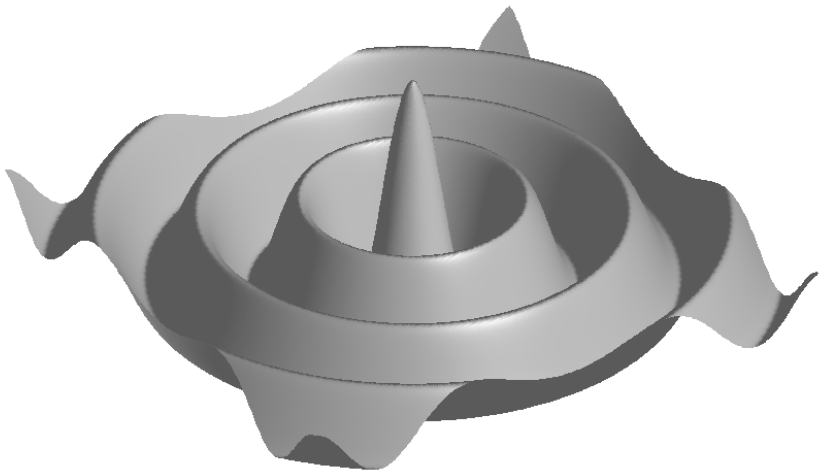

Figure 5: Bessel function

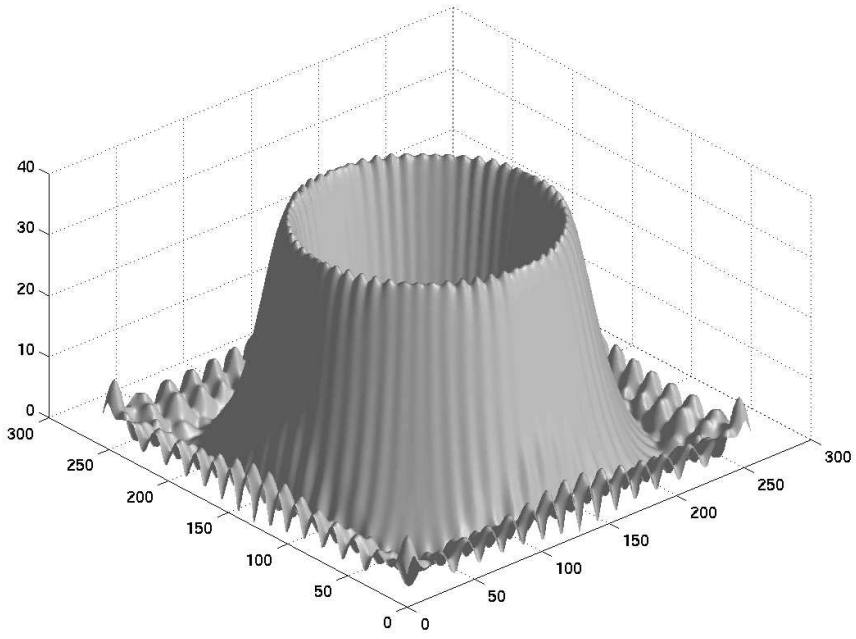

Figure 6: Siemens-star convolved with a spherical quadrature filter (magnitude)

In figure 7 the output of a spherical quadrature filter applied to an impulse-line is displayed. The lower right image shows the combined imaginary parts which means

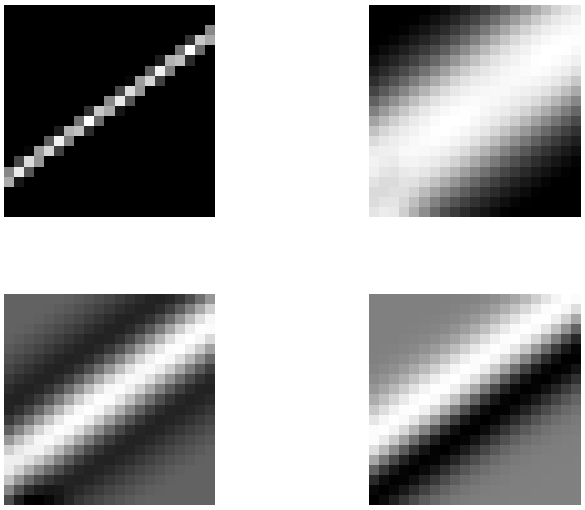

Figure 7: Upper left: impulse-line, upper right: amplitude of filter output, lower left: real part of filter output, lower right: combined imaginary parts of filter output

that it is simply the imaginary part of the 'correct' imaginary plane (that one which is obtained from the orientation phase).

Same as for 1D signals, 2D signals can be embedded as a surface in 3D space. The signal values are assigned to the real axis and the spatial coordinates to the $\boldsymbol{i}$- and the $\boldsymbol{j}$-axis. The spherical analytic signal can be represented in the same embedding. It corresponds to a vector field, which is only non-zero in the plane spanned by $\boldsymbol{i}$ and $\boldsymbol{j}$ (see figure 8).

As in the 1D case, the vector field looks like particles which roll from a ridge (impulse-line). The rotation is directed orthogonal away from the ridge and the speed decreases with increasing distance.

The result of filtering a signal with a spherical quadrature filter is a quaternion-valued field. Though the bivector (or $\boldsymbol{k}$) component of the field is always zero, we denote this field as a multivector field or the *structure multivector* of the signal.

As already the name induces, the structure multivector is closely related to the structure tensor. The structure tensor as defined in [10] includes the following information (in fact, only the orientation vector is considered):

- amplitude – measurement for the existence of local structure

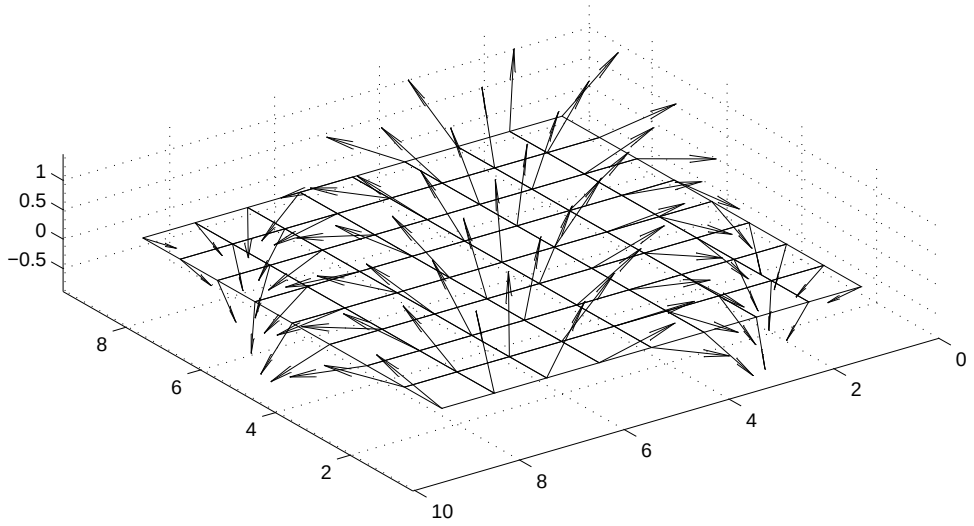

Figure 8: Representation of the spherical analytic signal as a vector field

- orientation – orientation of the local structure

Jähne [13] extracts an additional information: the coherence. The coherence is the relationship between the oriented gradients and all gradients, so it is a measurement for the degree of orientation in a structure and it is closely related to the variance of the orientation.

The variance is a second order property. It includes a product of the arguments and therefore, it is not linear. Consequently, the coherence cannot be measured by a linear approach like the structure multivector. Two structures with different orientations simply yield the vector sum of both multivector fields.

The structure multivector consists of three independent components (local phase, local orientation and local amplitude) and it codes three properties. Consequently, there is no additional information possible. The structure tensor possesses three degrees of freedom (it is a symmetric tensor) and codes only two properties. Therefore, one can additionally extract a third information, the coherence.

3.3 Detection of key points

The current status of our approach of detecting key points is not totally satisfying, because it is still nonlinear. The key idea is to calculate the *outer energy* of the multivector field. Outer energy means being contrary to the inner energy, which is calculated by the inner product of the multivectors. Obviously, this cannot be done pointwise, because the outer product of a multivector with itself is always zero[5].

Therefore, we consider a local neighborhood and in this local neighborhood we combine those areas which are assumed to have similar orientations. This is achieved as follows: the first vector for the outer product is obtained by convolving the signal with a cosine mask and the second one is obtained by convolving with a sine mask:

$$f_C(\boldsymbol{x}) = f_H(\boldsymbol{x}) * (\cos(\varphi_x) r(|\boldsymbol{x}|)) \tag{21}$$

$$f_S(\boldsymbol{x}) = f_H(\boldsymbol{x}) * (\sin(\varphi_x) r(|\boldsymbol{x}|)) \tag{22}$$

where $r(|\boldsymbol{x}|)$ is a function which is zero for $|\boldsymbol{x}| = 0$ and for large $|\boldsymbol{x}|$ (e.g. a shifted Gaussian function).

If we have an intrinsically 1D structure, both signals have the same phases. If we have a rectangular corner, they are orthogonal. Consequently, the outer product (cross product[6])

$$f_J(\boldsymbol{x}) = f_C(\boldsymbol{x}) \times f_S(\boldsymbol{x}) \tag{23}$$

is zero in the first case and is maximized in the second case.

[5]Note in this context, the inner product stands for the squared magnitude and the outer product is the cross product between the 3D component vectors obtained from the multivectors.

[6]In the formula, we use the notation of the cross product in order to distinguish between the algebras we work on (see also footnote 5).

4 Experiments and Discussion

This section shows some experiments and an implementation in MatLab. The results are compared to those which can be found in [10] for example.

4.1 Implementation and tests

Throughout this section we used the implementations which can be found in the appendix.

The function which computes the structure multivector uses a multi-scale approach, because the shift of the Gaussian bandpass is coupled with the variance as for the Gabor wavelets. Both functions are first implementations, which should only underline the practicability of the approach.

For testing the implementations, we chose some synthetic examples with letters as gray level or textured images.

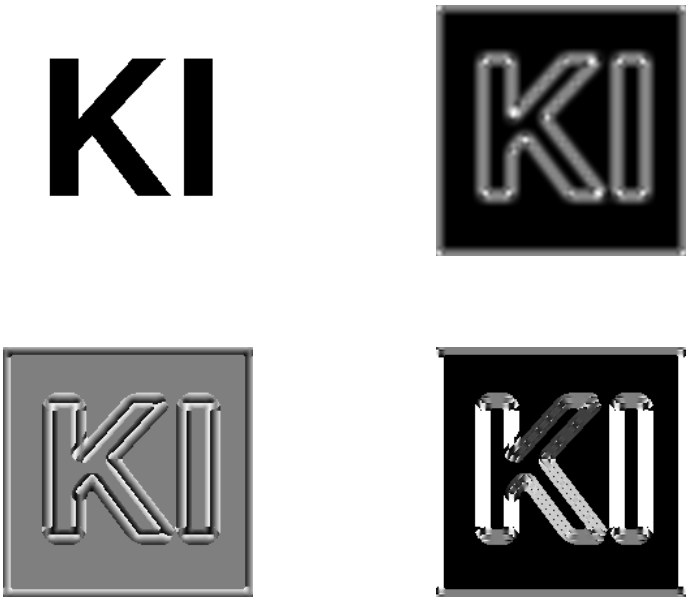

Figure 9: Structure multivector applied to an image without texture. Upper left: original, upper right: amplitude, lower left: φ_i-phase, lower right: φ_u-phase

In figure 9 it can be seen that the structure multivector responds only at the edges. Therefore, the amplitude is a measure for the presence of structure. The φ_i-phase is

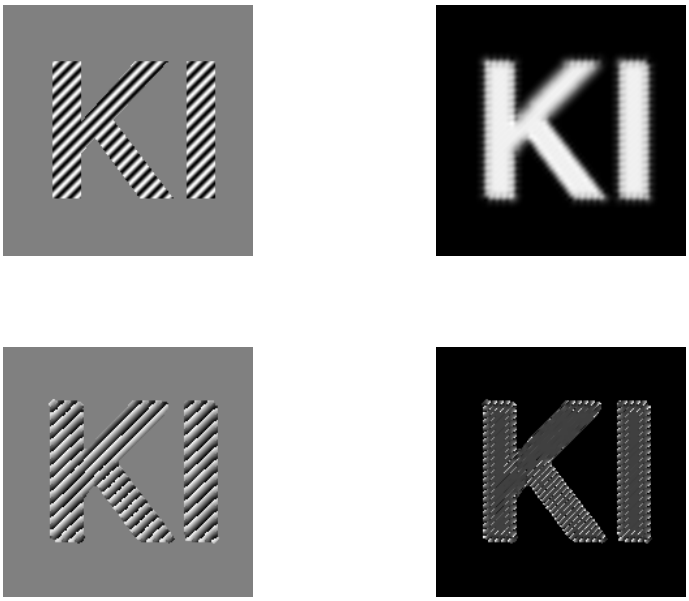

Figure 10: Structure multivector applied to an image with one texture. Upper left: original, upper right: amplitude, lower left: φ_i-phase, lower right: φ_u-phase

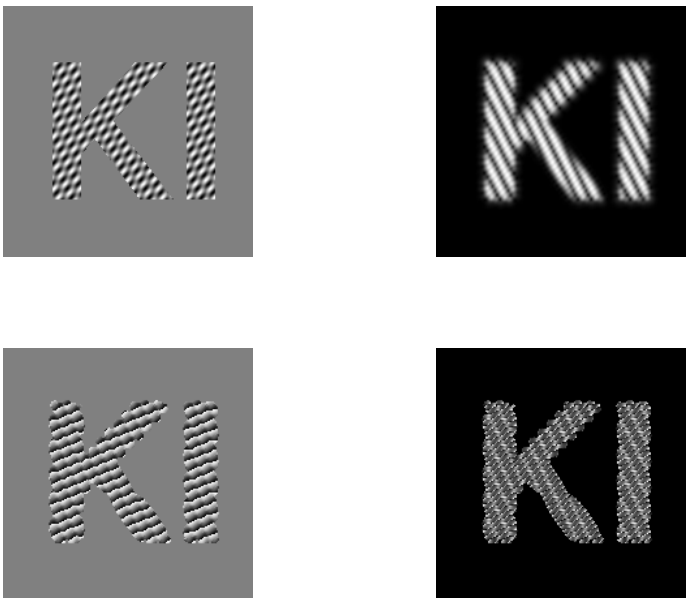

Figure 11: Structure multivector applied to an image with two superposed textures. Upper left: original, upper right: amplitude, lower left: φ_i-phase, lower right: φ_u-phase

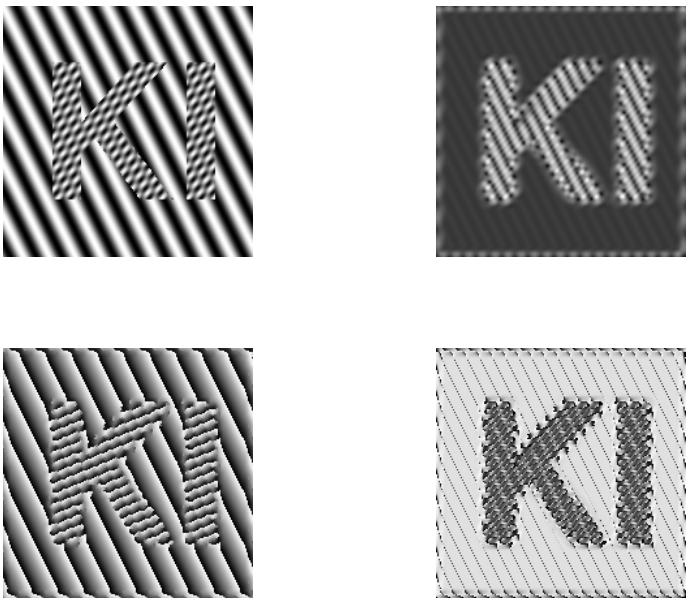

Figure 12: Structure multivector applied to an image with two superposed textures and textured background. Upper left: original, upper right: amplitude, lower left: φ_i-phase, lower right: φ_u-phase

linear, which can only be guessed in this representation. But it can be seen that the φ_i-phase is monotonic modulo a maximal interval (which is in fact 2π). The φ_u-phase represents the orientation of the edge. Note that the highest and the lowest gray level (standing for π and zero, respectively) represent the same orientation.

In figure 10 it can be seen that the structure multivector responds also inside the object. The amplitude is nearly constant, which corresponds to a texture with constant energy. Of course, this property is lost if the wrong scale is considered. The φ_i-phase is linear, see notes above. The φ_u-phase represents the orientation of the texture. A constant gray level corresponds to a constant estimated orientation. The small spikes in the figure are produced by the extraction of the local orientation angle. The underlying quaternion-valued field does not show these artifacts.

In figure 11 it can be seen that the structure multivector responds only with respect to the dominant texture. The magnitude of the response is modulated with that component of the weaker texture that is normal to the dominant texture. This effect is even more obvious in figure 12. The φ_i-phase is always directed parallel to the dominant texture. The φ_u-phase represents the orientation of the dominant texture in each case.

The described 2D detection algorithm works fine for images without texture. The amplitude of the detection filter response can be seen in figure 13. Obviously, the response increases with increasing sharpness of the corner.

Figure 13: Result of the 2D key-point detection applied to the multivector field from figure 9

4.2 Discussion of results

In contrast to the structure tensor which becomes zero for ideal 2D points (e.g. rectangular corner) the structure multivector responds at a high energy level. Therefore, it is easier to design a detector for those points, because the energy is higher. Furthermore, a concept like the outer energy does not produce artificial double lines beneath the original edges. These double lines makes it necessary to use a normalized convolution. Our approach does not need such tricks to obtain clear cut results.

4.3 Future work

In our future work, we will try to linearize the 2D key point detection. This will be done in an 8D algebra. Furthermore, we will try to separate texture information from edge information in a second filtering step, using the same algebra. Up to now, textures which are not parallel to the edge produce artificial 2D key points. The long-term objective will be the design of filters which covers the entire hierarchy of intrinsic dimensionality, consisting of (1D and 2D) textures, edges, corners and planes.

Another extension of the presented theory will be the consideration of higher dimensional cases, especially the image sequence analysis. The approach of the spherical analytic signal can be extended to higher dimensions easily.

The theoretical background will be further investigated with regard to the results from Clifford analysis, especially the monogenic function and other multidimensional generalizations of the analytic function.

Appendix

MatLab function for computing the structure multivector

```
function[M]=str_mw(R,sigma,c);
% computes the structure multivector of a real signal R with a
% spherical quadrature filter with Gaussian bandpass
% sigma^2: variance, c: ratio of waves
if nargin<3,
  c=0.5;
end;
s=size(R,1);
sh=s/2;
sig2=2*sigma;
[u,v]=meshgrid([-sh:sh-1],[-sh:sh-1]);
a=sqrt(u.^2+v.^2);
g=exp(-2*(pi*(a/s*sigma-c)).^2)*sigma*sqrt(2*pi);
g(sh+1,sh+1)=0;
N=fftshift(ifft2(ifftshift(g)));
N=N(sh+1-sig2:sh+sig2,sh+1-sig2:sh+sig2);
a(sh+1,sh+1)=1;
g=g./a;
u=u.*g;
v=v.*g;
U=fftshift(ifft2(ifftshift(u)));
V=fftshift(ifft2(ifftshift(v)));
U=U(sh+1-sig2:sh+sig2,sh+1-sig2:sh+sig2);
V=V(sh+1-sig2:sh+sig2,sh+1-sig2:sh+sig2);
M(:,:,2)=conv2(R,-imag(U),'same');
M(:,:,3)=conv2(R,-imag(V),'same');
M(:,:,1)=conv2(R,real(N),'same');
```

MatLab function for detecting intrinsically 2D structures

```
function[C]=detect2d(M,bd_m,bd_w);
% detection of 2D key-points with radial log-normal weighting
[u,v]=meshgrid([-4:4],[-4:4]);
m=sqrt(u.^2+v.^2);
m(5,5)=1;
bp=exp(-bd_w*log(m/bd_m).^2/log(2))./m;
bp(5,5)=0;
u=u.*bp;
v=v.*bp;
dc=conv2(M(:,:,1),u,'same');
ds=conv2(M(:,:,1),v,'same');
ec=conv2(M(:,:,2),u,'same');
es=conv2(M(:,:,2),v,'same');
fc=conv2(M(:,:,3),u,'same');
fs=conv2(M(:,:,3),v,'same');
a=ec.*fs-es.*fc;
b=ds.*fc-dc.*fs;
c=dc.*es-ds.*ec;
C=a.^2+b.^2+c.^2;
```

References

[1] BRACEWELL, R. N. *Two-Dimensional Imaging*. Prentice Hall signal processing series. Prentice Hall, Englewood Cliffs, 1995.

[2] BRACKX, F., DELANGHE, R., AND SOMMEN, F. *Clifford Analysis*. Pitman, Boston, 1982.

[3] BRADY, J. M., AND HORN, B. M. P. Rotationally symmetric operators for surface interpolation. *Computer Vision, Graphics, and Image Processing 22*, 1 (April 1983), 70–94.

[4] BÜLOW, T. *Global and Local Hypercomplex Spectral Signal Representations for Image Processing and Analysis*. PhD thesis, Christian-Albrechts-University of Kiel, 1999.

[5] DAVENPORT, C. M. A Commutative Hypercomplex Algebra with Associated Function Theory. In *Clifford Algebras with Numeric and Symbolic Computations*, R. Ablamowicz, Ed. Birkhäuser Bosten, 1996, pp. 213–227.

[6] ELL, T. A. *Hypercomplex Spectral Transformations*. PhD thesis, University of Minnesota, 1992.

[7] ERNST, R. R., AUE, W. P., BACHMANN, P., KARHAN, J., KUMAR, A., AND MÜLLER, L. Two-dimensional NMR spectroscopy. In *Proc. 4th Ampère Int. Summer School, Pula, Yugoslavia* (1976).

[8] FELSBERG, M., BÜLOW, T., AND SOMMER, G. Commutative Hypercomplex Fourier Transforms of Multidimensional Signals. In *Geometric Computing with Clifford Algebra*, G. Sommer, Ed. Springer, Heidelberg, 2000. to appear.

[9] GRANLUND, G. H. Hierarchical computer vision. In *Proc. of EUSIPCO-90, Fifth European Signal Processing Conference, Barcelona* (1990), L. Torres, E. Masgrau, and M. A. Lagunas, Eds., pp. 73–84.

[10] GRANLUND, G. H., AND KNUTSSON, H. *Signal Processing for Computer Vision*. Kluwer Academic Publishers, Dordrecht, 1995.

[11] HAGLUND, L. *Adaptive Multidimensional Filtering*. PhD thesis, Linköping University, 1992.

[12] HESTENES, D., AND SOBCZYK, G. *Clifford algebra to geometric calculus, A Unified Language for Mathematics and Physics*. Reidel, Dordrecht, 1984.

[13] JÄHNE, B. *Digitale Bildverarbeitung*. Springer, Berlin, 1997.

[14] KARLHOLM, J. *Local Signal Models for Image Sequence Analysis*. PhD thesis, Linköping University, 1998.

[15] MERRON, J., AND BRADY, M. Isotropic gradient estimation. In *IEEE Computer Vision and Pattern Recognition* (1996), pp. 652–659.

[16] MICHAELIS, M., AND SOMMER, G. A Lie group approach to steerable filters. *Pattern Recognition Letters 16* (1995), 1165–1174.

[17] NABIGHIAN, M. N. Toward a three-dimensional automatic interpretation of potential field data via generalized Hilbert transforms: Fundamental relations. *Geophysics 49*, 6 (June 1984), 780–786.

[18] SOMMER, G. The global algebraic frame of the perception-action cycle. In *Handbook of Computer Vision and Applications* (1999), B. Jähne, H. Haußecker, and P. Geissler, Eds., vol. 3, Academic Press, San Diego, pp. 221–264.

[19] STEIN, E., AND WEISS, G. *Introduction to Fourier Analysis on Euclidean Spaces*. Princeton University Press, New Jersey, 1971.

[20] YU, W., DANIILIDIS, K., BEAUCHEMIN, S., AND SOMMER, G. Detection and characterization of multiple motion points. In *18th IEEE conference on Computer Vision and Pattern Recognition, Fort Collins, Colorado* (1999).